Guide to Compact Approximate Taylor methods for hyperbolic systems

C. Parés

Universidad de Málaga

Seminario EDANYA, 5 November 2021

Outline

- The ingredients of high-order Lax-Wendroff-type methods for linear systems are:
  - Taylor expansions to advance in time;
  - time derivatives are transformed into spatial derivatives using the equation;
  - centered numerical differentiation formulas are used to approximate spatial derivatives.

- The ingredients of high-order Lax-Wendroff-type methods for linear systems are:
  - Taylor expansions to advance in time;
  - time derivatives are transformed into spatial derivatives using the equation;
  - centered numerical differentiation formulas are used to approximate spatial derivatives.

- The main difficulty to extend them to nonlinear systems of conservation laws is the transformation of time derivatives in spatial derivatives. Some strategies:
  - Cauchy-Kovalevskaya (**CK**) procedure: Qiu and Shu (2003) ...
  - Generalized Riemann problems: ADER methods: Titarev and Toro (2002) ...
  - Local time-space problems:
    - ADER-WENO methods C. Enaux, M. Dumbser and E.F. Toro (2008)...
    - $P_N P_M$ methods: M. Dumbser, D. Balsara, E.F. Toro and C.D. Munz (2008) ...
  - Approximate Taylor (**AT**) method: **LAT** method Zorío, Baeza and Mulet (2017)...

The goals of this work are the following:

1. To develop a family of high-order numerical methods for nonlinear systems of conservation laws based on approximate Taylor **AT** procedures that constitute a proper generalization of Lax-Wendroff methods, i.e. that reduce to the standard high-order Lax-Wendroff methods when the flux is linear.

The goals of this work are the following:

1. To develop a family of high-order numerical methods for nonlinear systems of conservation laws based on approximate Taylor **AT** procedures that constitute a proper generalization of Lax-Wendroff methods, i.e. that reduce to the standard high-order Lax-Wendroff methods when the flux is linear.
2. To combine this new **AT** procedure with shock-capturing techniques to cure the spurious oscillations generated close to discontinuities by the **AT** methods.

The goals of this work are the following:

1. To develop a family of high-order numerical methods for nonlinear systems of conservation laws based on approximate Taylor **AT** procedures that constitute a proper generalization of Lax-Wendroff methods, i.e. that reduce to the standard high-order Lax-Wendroff methods when the flux is linear.
2. To combine this new **AT** procedure with shock-capturing techniques to cure the spurious oscillations generated close to discontinuities by the **AT** methods.
3. To extend the methods to system of balance laws to obtain high-order well-balanced numerical methods.

The goals of this work are the following:

1. To develop a family of high-order numerical methods for nonlinear systems of conservation laws based on approximate Taylor **AT** procedures that constitute a proper generalization of Lax-Wendroff methods, i.e. that reduce to the standard high-order Lax-Wendroff methods when the flux is linear.
2. To combine this new **AT** procedure with shock-capturing techniques to cure the spurious oscillations generated close to discontinuities by the **AT** methods.
3. To extend the methods to system of balance laws to obtain high-order well-balanced numerical methods.

Conjoint work with H. Carrillo, G. Russo, E. Macca, D. Zorío.

Outline

In 1960 P.D. Lax and B. Wendroff proposed a numerical technique for solving approximately systems of hyperbolic conservation laws: the explicit second-order Lax-Wendroff method.
Let us consider the scalar linear transport equation

$$u_t + a u_x = 0,$$

where a is constant. The derivation of the method is based on the second-degree Taylor expansion:

$$u(x_i, t^{n+1}) = u(x_i, t^n) + \Delta t \partial_t u(x_i, t^n) + \frac{\Delta t^2}{2} \partial_t^2 u(x_i, t^n) + O(\Delta t^3). \quad (1)$$

Then, assuming that the solution is smooth, one can replace time derivatives by spatial derivatives using the equation:

$$\partial_t u(x,t) = -a \partial_x u(x,t), \quad \partial_t^2 u(x,t) = a^2 \partial_x^2 u(x,t).$$

Finally, the spatial derivatives are approximated by centered 3-point formulas of numerical differentiation:

$$\begin{aligned} \partial_x u(x_i, t_n) &\cong \frac{1}{2\Delta x}(u(x_{i+1}, t_n) - u(x_{i-1}, t_n)), \\ \partial_x^2 u(x_i, t_n) &\cong \frac{1}{\Delta x^2}(u(x_{i+1}, t_n) - 2u(x_i, t_n) + u(x_{i-1}, t_n)) \end{aligned}$$

what leads to the Lax-Wendroff LW method:

$$u_i^{n+1} = u_i^n - \frac{a\Delta t}{2\Delta x}(u_{i+1}^n - u_{i-1}^n) + \frac{a^2\Delta t^2}{2\Delta x^2}(u_{i+1}^n - 2u_i^n + u_{i-1}^n). \tag{2}$$

A uniform mesh with nodes $\{x_i\}$ and step Δx is considered. As usual, u_i^n represents the approximation of the the solution at x_i at time $t^n = n\Delta t$, where Δt is the time step.

The method can be written in conservative form:

$$u_i^{n+1} = u_i^n - \frac{\Delta t}{\Delta x}(F_{i+1/2} - F_{i-1/2}), \tag{3}$$

where

$$F_{i+1/2} = \frac{a}{2}(u_i^n + u_{i+1}^n) - \frac{a^2\Delta t}{2\Delta x}(u_{i+1}^n - u_i^n). \tag{4}$$

The scheme is second-order accurate and L^2 stable under the CFL condition

$$|c| \leq 1, \quad c = \frac{a\Delta t}{\Delta x}.$$

The method can be easily extended to high-order: the m-degree Taylor expansion is first considered.

$$u(x_i, t^{n+1}) = u(x_i, t^n) + \sum_{k=1}^{m} \frac{\Delta t^k}{k!} \partial_t^k u(x_i, t^n) + O(\Delta t^{m+1}). \tag{5}$$

Time derivatives are replaced by space derivatives then through the identities

$$\partial_t^k u = (-1)^k a^k \partial_x^k u, \quad k = 1, 2 \ldots \tag{6}$$

Finally, centered $(2p+1)$-point numerical differentiation formulas are used to approximate the spatial derivatives:

$$u_i^{n+1} = u_i^n + \sum_{k=1}^{m} \frac{(-1)^k c^k}{k!} \sum_{j=-p}^{p} \delta_{p,j}^k \, u_{i+j}^n, \tag{7}$$

where:

- p, m are natural numbers;
- $c = a\Delta t/\Delta x$;
- $\delta_{p,j}^k$ are the coefficients of the $(2p+1)$-point centered interpolatory formula of numerical differentiation

$$f^{(k)}(x_i) \simeq D_{p,i}^k(f, \Delta x) = \frac{1}{\Delta x^k} \sum_{j=-p}^{p} \delta_{p,j}^k f(x_{i+j}). \tag{8}$$

The resulting numerical method can be written in conservative form. To do so, a new family of $(2p)$-point formula of numerical differentiation:

$$f^{(k)}(x_i + q\Delta x) \simeq A^{k,q}_{p,i}(f, \Delta x) = \frac{1}{\Delta x^k} \sum_{j=-p+1}^{p} \gamma^{k,q}_{p,j} f(x_{i+j}), \tag{9}$$

has to be introduced. $A^{k,q}_{p,i}(f, \Delta x)$ is the numerical differentiation formula that approximates the k-th derivative at the point $x_i + q\Delta x$ using the values of the function at the $2p$ points $x_{i-p+1}, \ldots, x_{i+p}$.

Observe that the coefficients, like in (8), do not depend on i. Following Fornberg, (1998) iterative formulas to compute the coefficients $\delta^k_{p,j}$ have been derived.

Given a variable w, the following notation will be used:

$$\begin{aligned} D^k_{p,i}(w_*, \Delta x) &= \frac{1}{\Delta x^k} \sum_{j=-p}^{p} \delta^k_{p,j} w_{i+j}, \\ A^{k,q}_{p,i}(w_*, \Delta x) &= \frac{1}{\Delta x^k} \sum_{j=-p+1}^{p} \gamma^{k,q}_{p,j} w_{i+j}, \end{aligned}$$

to indicate that the formulas are applied to the approximations of w, w_i, and not to its exact point values $w(x_i)$.

The equality:

$$D_{p,i}^{k+1}(f,\Delta x) = \frac{1}{\Delta x}\left(A_{p,i}^{k,1/2}(f,\Delta x) - A_{p,i-1}^{k,1/2}(f,\Delta x)\right)$$

holds.

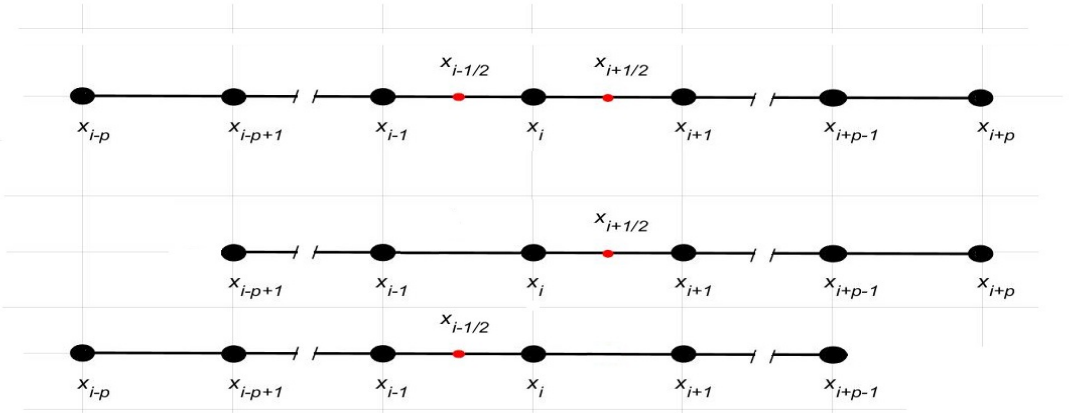

This equality allows us to write the numerical method (7) in conservative form:

$$u_i^{n+1} = u_i^n + \frac{\Delta t}{\Delta x}\left(F_{i-1/2}^p - F_{i+1/2}^p\right), \tag{10}$$

with,

$$F_{i+1/2}^p = \sum_{k=1}^{2p}(-1)^{k-1}\frac{a^k \Delta t^{k-1}}{k!}A_{p,i}^{k-1,1/2}(u_*^n, \Delta x). \tag{11}$$

Example: for $p = 2$, the fourth-order numerical flux is:

$$\begin{aligned} F_{i+1/2}^2 \quad = \quad & \frac{a}{12}(-u_{i-1}^n + 7u_i^n + 7u_{i+1}^n - u_{i+2}^n) + \frac{a^2\Delta t}{24\Delta x}(-u_{i-1}^n + 15u_i^n - 15u_{i+1}^n + u_{i+2}^n) \\ & + \frac{a^3\Delta t^2}{12\Delta x^2}(u_{i-1}^n - u_i^n - u_{i+1}^n + u_{i+2}^n) + \frac{a^4\Delta t^3}{24\Delta x^3}(u_{i-1}^n - 3u_i^n + 3u_{i+1}^n - u_{i+2}^n), \end{aligned}$$

The accuracy and stability of these methods have been studied in Carrillo and CP (2019) [1]: the numerical method is of order m in time and $2p$ in space. If $m = 2p$, the numerical method has order of accuracy $2p$ and it is L^2-stable under the CFL condition $|c| \leq 1$.

Outline

Let us consider first the one-dimensional scalar conservation law:

$$u_t + f(u)_x = 0. \tag{12}$$

As in the linear case, the second-degree Taylor expansion is first considered:

$$u(x_i, t^{n+1}) \approx u_i + \Delta t \partial_t u(x_i, t_n) + \frac{\Delta t^2}{2} \partial_t^2 u(x_i, t_n) + O(\Delta t^3). \tag{13}$$

In the CK procedure, time derivatives are transformed in space derivatives using the equation as follows:

$$\begin{aligned} \partial_t u &= -f(u)_x; \\ \partial_t^2 u &= f'(u) f(u)_{xx}. \end{aligned}$$

Numerical differentiation formulas are then applied to discretize the space derivative. For instance, in [8], Qiu and Shu (2003) WENO reconstructions are used to compute the first order derivative and centered formulas for the second one.

When applied to derive higher order methods, specially for systems of conservation laws, this procedure may require symbolic calculus. Moreover, the number of terms in the expression of the derivatives and the stencil increases with the order.

In [9], Zorio, Mulet and Baeza (2017) introduced a technique that avoids the CK procedure, in which time derivatives are transformed in space derivatives using the equalities:

$$\begin{aligned} \partial_t u &= -f(u)_x, \\ \partial_t^2 u &= -\partial_x \partial_t f(u). \end{aligned}$$

The Algorithm is as follows: once the approximations $\{u_i^n\}$ at time t^n have been computed

- Define $f_i^{(0)} = f_i^n = f(u_i^n), \forall i.$ $\quad f_i^{(0)} \approx f(u(x_i, t_n))$
- Compute $u_i^{(1)} = -\dfrac{f_{i+1}^{(0)} - f_{i-1}^{(0)}}{2\Delta x}, \forall i.$ $\quad u_i^{(1)} \approx \partial_t u(x_i, t_n)$
- Compute $f_i^{n+1} = f\left(u_i^n + \Delta t\, u_i^{(1)}\right), \forall i.$ $\quad f_i^{n+1} \approx f(u(x_i, t^{n+1}))$
- Compute $f_i^{n-1} = f\left(u_i^n - \Delta t\, u_i^{(1)}\right), \forall i.$ $\quad f_i^{n-1} \approx f(u(x_i, t^{n-1}))$
- Compute $f_i^{(1)} = \dfrac{f_i^{n+1} - f_i^{n-1}}{2\Delta t}, \forall i.$ $\quad f_i^{(1)} \approx \partial_t f(u)(x_i, t_n)$
- Compute $u_i^{(2)} = -\dfrac{f_{i+1}^{(1)} - f_{i-1}^{(1)}}{2\Delta x}, \forall i.$ $\quad u_i^{(2)} \approx \partial_t^2 u(x_i, t_n)$
- Update: $u_i^{(n+1)} = u_i^n + \Delta t\, u_i^{(1)} + \dfrac{\Delta t^2}{2} u_i^{(2)}, \forall i.$

- In Zorio, Mulet and Baeza (2017) [9] WENO reconstructions are used to compute $\tilde{u}_i^{(1)}$ like in Qui-Shu method to cure oscillations.
- Observe that Taylor expansions are used to approximate $f(u(x_i, t^{n+1}))$ and $f(u(x_i, t^{n-1}))$. Once these approximations have been computed, the centered 3-point formula of numerical differentiation is used to approximate the time derivative of $f(u)$.
- It would be possible to use $f(u_i^{n-1})$ as an approximation of $f(u(x_i, t^{n-1}))$, but then the method would be multistep in time.
- This method is is not a generalization of LW (5): if $f(u) = au$, it can be easily checked that the method writes as follows

$$u_i^{n+1} = u_i^n - \frac{c}{2}(u_{i+1}^n - u_{i-1}^n) + \frac{c^2}{8}(u_{i+2}^n - 2u_i^n + u_{i-2}^n). \qquad (14)$$

This method uses 5-point stencils instead of 3-point ones and the stability properties are worse.

In [1], Carrillo and CP (2019) introduced a variant that reduces LW when applied to the linear flux $f(u) = au$. The idea is as follows: the second-order Approximate Taylor method writes as follows:

$$u_i^{n+1} = u_i^n - \Delta t \frac{f_{i+1}^{(0)} - f_{i-1}^{(0)}}{2\Delta x} - \frac{\Delta t^2}{2} \frac{f_{i+1}^{(1)} - f_{i-1}^{(1)}}{2\Delta x}.$$

This method can be written in conservation form with numerical flux

$$F_{i+1/2} = \frac{1}{2}\left(f_i^{(0)} + f_{i+1}^{(0)}\right) + \frac{\Delta t}{4}\left(f_i^{(1)} + f_{i+1}^{(1)}\right).$$

The idea in CAT method is to compute this numerical flux using only the numerical approximations u_i^n, u_{i+1}^n what ensures that the stencil consists of the three nodes: x_{i-1}, x_i, x_{i+1}.

To do so, local approximations

$$f_{i,0}^{(1)} \approx \partial_t f(u)(x_i, t_n), \quad f_{i,1}^{(1)} \approx \partial_t f(u)(x_{i+1}, t_n),$$

will be computed. They are local in the sense that, in general

$$f_{i,1}^{(1)} \neq f_{i+1,0}^{(1)}.$$

The Algorithm is as follows: once $\{u_i^n\}$, have been computed

- For all i:
  - Define $f_{i,j}^{(0)} = f_{i,j}^n = f(u_{i+j}^n), \quad j = 1, 2.$ $\quad f_{i,j}^{(0)} \approx f(u(x_{i+j}, t_n))$
  - Compute $u_{i,j}^{(1)} = -\dfrac{f_{i,1}^{(0)} - f_{i,0}^{(0)}}{\Delta x}, \quad j = 1, 2.$ $\quad u_{i,j}^{(1)} \approx \partial_t u(x_{i+j}, t_n)$
  - Compute $f_{i,j}^{n+1} = f\left(u_{i+j}^n + \Delta t\, u_{i,j}^{(1)}\right), \quad j = 1, 2.$ $\quad f_{i,j}^{n+1} \approx f(u(x_{i+j}, t^{n+1}))$
  - Compute $f_{i,j}^{(1)} = \dfrac{f_{i,j}^{n+1} - f_{i,j}^n}{\Delta t}, \quad j = 1, 2.$ $\quad f_{i,j}^{(1)} \approx \partial_t f(u)(x_{i+j}, t_n)$
  - Compute

$$F_{i+1/2}^1 = \frac{1}{2}\left(f_{i,0}^{(0)} + f_{i,1}^{(0)}\right) + \frac{\Delta t}{4}\left(f_{i,0}^{(1)} + f_{i,1}^{(1)}\right) = \frac{1}{4}\left(f_{i,0}^n + f_{i,1}^n + f_{i,0}^{n+1} + f_{i,1}^{n+1}\right).$$

- For all i compute $u_i^{n+1} = u_i^n - \dfrac{\Delta t}{\Delta x}\left(F_{i+1/2}^1 - F_{i-1/2}^1\right).$

It is second-order accurate and it reduces to LW when $f(u) = au$. Therefore, it is linearly L^2-stable under the usual CFL condition.

Extension to nonlinear systems: CAT2 method

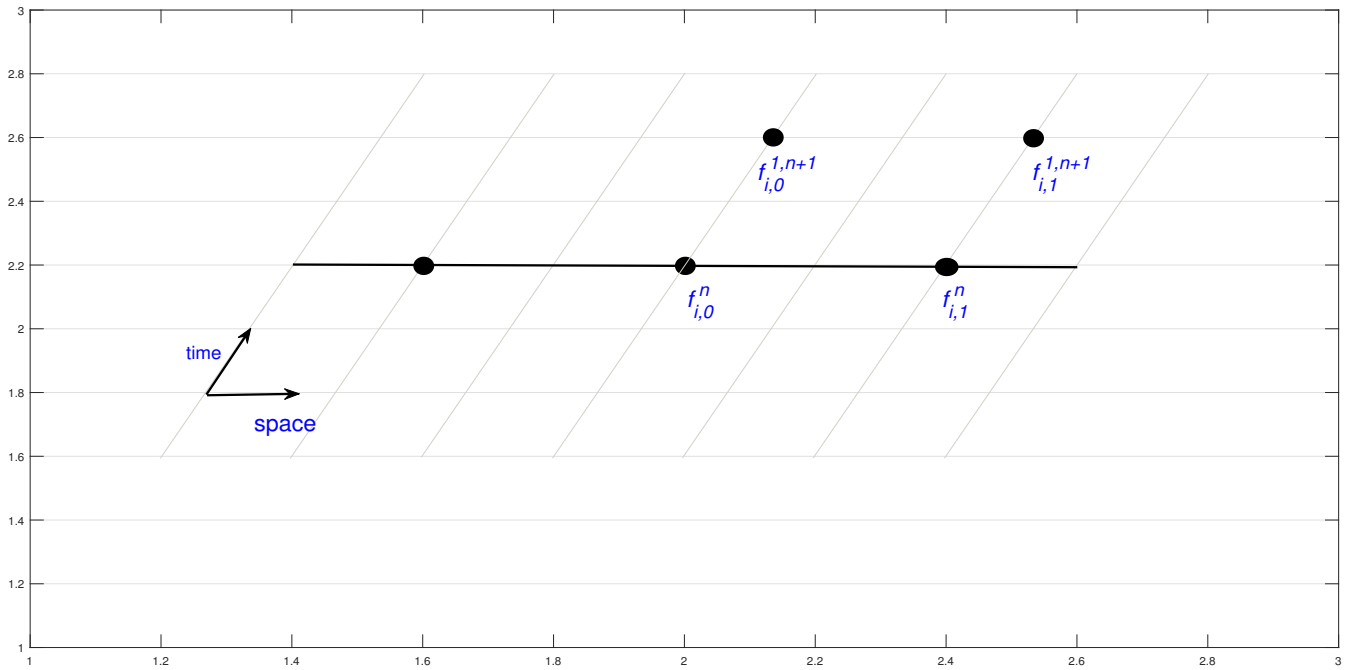

Outline

The numerical flux $F^p_{i+1/2}$ of the CAT2p method will be computed using only the approximations

$$u^n_{i-p+1}, \ldots, u^n_{i+p}, \tag{15}$$

so that the values used to update u^{n+1}_i are only those of the centered $(2p+1)$-point stencil, like in the linear case.

The symbol $*$ will be used to indicate the index with respect to which the differentiation is taken. For instance:

$$\partial^k_x u(x_i + q\Delta x, t_n) \simeq A^{k,q}_{p,i}(u^n_*, \Delta x) = \frac{1}{\Delta x^k} \sum_{j=-p+1}^{p} \gamma^{k,q}_{p,j} u^n_{i+j},$$

$$\partial^k_t u(x_i, t_n + q\Delta t) \simeq A^{k,q}_{p,n}(u^*_i, \Delta t) = \frac{1}{\Delta t^k} \sum_{r=-p+1}^{p} \gamma^{k,q}_{p,r} u^{n+r}_i.$$

Once the approximations $\{u_i^n\}$ have been computed:

- For all i:
  - Compute $f_{i,j}^{(0)} = f(u_{i+j}^n), \quad j = -p+1, \ldots, p.$
  - For $k = 2 \ldots 2p$:
    - Compute
    $$u_{i,j}^{(k-1)} = -A_{p,0}^{1,j}(f_{i,*}^{(k-2)}, \Delta x).$$
    - Compute
    $$f_{i,j}^{k-1,n+r} = f\left(u_{i+j}^n + \sum_{l=1}^{k-1} \frac{(r\Delta t)^l}{l!} u_{i,j}^{(l)}\right), \quad j, r = -p+1, \ldots, p.$$
    - Compute
    $$f_{i,j}^{(k-1)} = A_{p,n}^{k-1,0}(f_{i,j}^{k-1,*}, \Delta t), \quad j = -p+1, \ldots, p.$$
  - Compute
  $$F_{i+1/2}^p = \sum_{k=1}^{2p} \frac{\Delta t^{k-1}}{k!} A_{p,0}^{0,1/2}(\tilde{f}_{i,*}^{(k-1)}, \Delta x).$$
- Update
$$u_i^{n+1} = u_i^n - \frac{\Delta t}{\Delta x}\left(F_{i+1/2}^p - F_{i-1/2}^p\right).$$

In Carrillo and CP (2019) [1] the following result has been proved:

Theorem

For every p, CAT2p is $2p$-order accurate and it reduces to the $2p$-order Lax-Wendroff scheme (5) when $f(u) = au$.

- The extension of LAT methods to order $2p$ uses $(4p+1)$-stencil and has worse stability properties than CAT.
- Every time iteration of CAT is costly that LAT due to the local approximations. Nevertheless, this extra cost may be compensanted by the fact that larger time steps can be chosen.

Let us consider the scalar transport equation $u_t + u_x = 0$, in the spatial interval $[0, 1]$, the initial condition

$$u(x,0) = \begin{cases} 1 & 0 \leq x < 2/10, \\ 2 & 2/10 \leq x < 7/10, \\ 1 & 7/10 \leq x < 1, \end{cases} \tag{16}$$

periodic boundary conditions, a uniform mesh with $N = 80$ points, $CFL = 0.9$ and $t = 1$. The CAT method (that, in this case, coincides with the Lax-Wendroff method) is applied for $p = 1, \ldots, 5$.

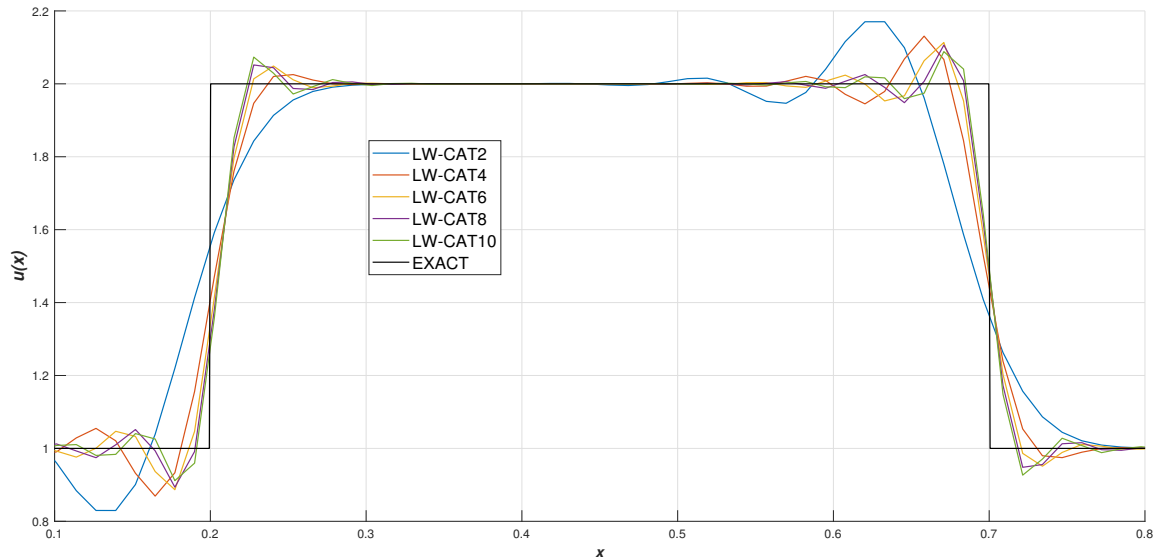

Let us consider now Burgers equation

$$u_t + \left(\frac{u^2}{2}\right)_x = 0$$

with the same initial condition and periodic boundary conditions.
CAT2p, $p = 1, 2, 3, 4$ are applied to the problem using a grid of 80-point mesh and $t = 1.2$s. The numerical solutions that are oscillatory but remain stable for CFL values that decrease with the other CFL$= 0.8, 0.4, 0.2, 0.1$.

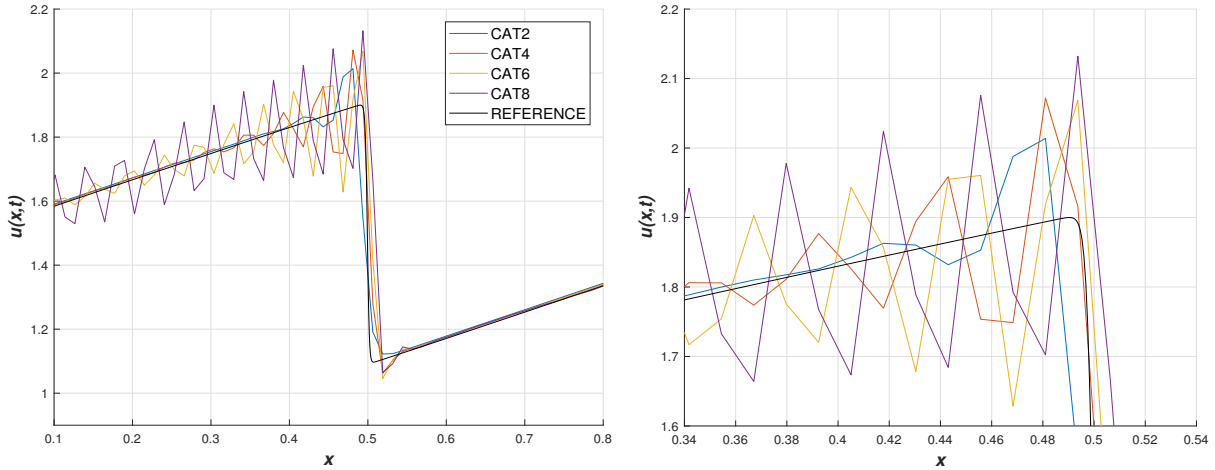

ACAT methods have been extended to systems of balance laws

$$u_t + f(u)_x = S(u)H_x, \tag{17}$$

where H is a known function.

The strategy is to rewrite the systems as

$$u_t + F(u)_x = 0,$$

with the 'augmented flux'

$$F(u(x,t)) = f(u(x,t)) - \int_{-\infty}^{x} S(u(s,t))H_x(s)\,ds$$

and apply ACAT methods to this reformulation.

The Algorithm is as follows: once $\{u_i^n\}$, have been computed

- For all i:
  - Define $f_{i,j}^{(0)} = f_{i,j}^n = f(u_{i+j}^n), \quad j = 1, 2.$
  - Compute

$$u_{i,j}^{(1)} = -\frac{f_{i,1}^{(0)} - f_{i,0}^{(0)}}{\Delta x} + \frac{1}{2}\left(S(u_i^n)H_x(x_i) + S(u_{i+1}^n)H_x(x_{i+1})\right), \quad j = 1, 2.$$

  - Compute $f_{i,j}^{n+1} = f\left(u_{i+j}^n + \Delta t\, u_{i,j}^{(1)}\right), \quad j = 1, 2.$
  - Compute $F_{i+1/2}^1 = \frac{1}{4}\left(f_{i,0}^n + f_{i,1}^n + f_{i,0}^{n+1} + f_{i,1}^{n+1}\right).$
- For all i:
  - Compute:

$$\begin{aligned} S_i^1 \quad := \quad & \frac{\Delta x}{8}\Big((S(u_{i-1}^n) + S(u_{i-1,0}^{1,n+1}))H_x(x_{i-1}) + (S(u_i^n) + S(u_{i-1,1}^{1,n+1}))H_x(x_i) \\ & + (S(u_i^n) + S(u_{i,0}^{1,n+1}))H_x(x_i) + (S(u_{i+1}^n) + S(u_{i,1}^{1,n+1}))H_x(x_{i+1})\Big). \end{aligned}$$

  - Update $u_i^{n+1} = u_i^n - \frac{\Delta t}{\Delta x}\left(F_{i+1/2}^1 - F_{i-1/2}^1 + S_i^1\right).$

Well-balanced versions have been also implemented. The idea is as follows: if u^* is a stationary solution of the problem, i.e

$$F(u^*) = S(u^*)H_x,$$

such that $u^*(x) = u(x,t)$ then, at (x,t) the equation can be equivalently rewritten as

$$u_t + \widetilde{F}(u)_x = 0,$$

where

$$\widetilde{F}(u(x,t)) = f(u(x,t)) - f(u^*(x)) - \int_{-\infty}^{x} \left(S(u(s,t)) - S(u^*(s))\right) H_x(s)\, ds.$$

ACAT methods are then applied to this formal conservative expression. Observe that $\widetilde{F}(u(x,t)) = 0$ if $u \equiv u^*$.

For all i:

- Compute the stationary solution u_i^* that satisfies $u_i^*(x_i) = u_i^n$.
- For $j = 0, 1$ compute

$$u_{i;i,j}^{(1)} = -\frac{1}{\Delta x}\Big(f(u_{i+1}^n) - f(u_i^n) - f(u_i^*(x_{i+1})) + f(u_i^*(x_i))\Big)$$
$$+\frac{1}{2}\Big((S(u_i^n) - S(u_i^*(x_i)))H_x(x_i) + (S(u_{i+1}^n) - S(u_i^*(x_{i+1})))H_x(x_{i+1})\Big);$$
$$u_{i;i-1,j}^{(1)} = -\frac{1}{\Delta x}\Big(f(u_i^n) - f(u_{i-1}^n) - f(u_i^*(x_i)) + f(u_i^*(x_{i-1}))\Big)$$
$$+\frac{1}{2}\Big((S(u_{i-1}^n) - S(u_i^*(x_{i-1})))H_x(x_{i-1}) + (S(u_i^n) - S(u_i^*(x_i)))H_x(x_i)\Big).$$

- Compute

$$u_{i;i,j}^{1,n+1} = u_{i+j}^n + \Delta t\ u_{i;i,j}^{(1)}, \quad j = 0, 1,$$
$$u_{i;i-1,j}^{1,n+1} = u_{i+j}^n + \Delta t\ u_{i-1;i,j}^{(1)}, \quad j = 0, 1.$$

- Compute

$$F^1_{i,i+1/2} := \frac{1}{4}\Big(f(u^n_i) + f(u^n_{i+1}) + f(u^{1,n+1}_{i;i,0}) + f(u^{1,n+1}_{i;i,1}) - 2f(u^*_i(x_i)) - 2f(u^*_i(x_{i+1}))\Big),$$

$$F^1_{i,i-1/2} := \frac{1}{4}\Big(f(u^n_{i-1}) + f(u^n_i) + f(u^{1,n+1}_{i;i-1,0}) + f(u^{1,n+1}_{i;i-1,1}) - 2f(u^*_i(x_{i-1})) - 2f(u^*_i(x_i))\Big),$$

$$\begin{aligned} S^1_i := \frac{\Delta x}{8}\Big(& (S(u^n_{i-1}) + S(u^{1,n+1}_{i-1,0}) - 2S(u^*_i(x_{i-1})))H_x(x_{i-1}) \\ & + (S(u^n_i) + S(u^{1,n+1}_{i;i-1,1}) - 2S(u^*_i(x_i)))H_x(x_i) \\ & + (S(u^n_i) + S(u^{1,n+1}_{i;i,0}) - 2S(u^*_i(x_i)))H_x(x_i) \\ & + (S(u^n_{i+1}) + S(u^{1,n+1}_{i;i,1}) - 2S(u^*_i(x_{i+1})))H_x(x_{i+1})\Big). \end{aligned}$$

- Update $u^{n+1}_i = u^n_i - \dfrac{\Delta t}{\Delta x}\left(F^1_{i,i+1/2} - F^1_{i,i-1/2} + S^1_i\right).$

Outline

Shock-capturing techniques

Three different shock-capturing technique have been considered so far to cure the oscillations close to discontinuities produced by CAT methods:

- WENO reconstructions: WENO-CAT methods.
- Flux Limiters: FL-CAT2.
- Adaptive compact approximate Taylor method: ACAT.

Following Zorio, Mulet and Baeza (2017), WENO reconstructions are used to compute the first-order time derivatives

$$\tilde{u}_{i,j}^{(1)} = -\frac{\hat{f}_{i+j+1/2} - \hat{f}_{i+j-1/2}}{\Delta x},$$

where $\hat{f}_{i+1/2}$ denotes the WENO reconstructions at $x_{i+1/2}$ of the flux function.

In Carrillo, CP, Zorío (2020) [3] CAT methods have been combined with fast-optimal versions of WENO.

Although the results are good, these methods have two drawbacks:

- while the order of CAT2p methods is even, that of WENO methods is odd;
- WENO method can spoil the good stability properties of CAT methods.

Numerical flux: convex combination of the CAT2 numerical flux $F^1_{i+1/2}$ and a first order robust numerical flux $F^L_{i+1/2}$:

$$F^*_{i+1/2} = (1 - \varphi^1_{i+1/2})F^L_{i+1/2} + \varphi^1_{i+1/2}F^1_{i+1/2}, \tag{18}$$

where $\varphi_{i+1/2}$ is a standard flux limiter function: Minmod, Superbee, Van Albada etc.

Numerical flux: convex combination of the CAT2 numerical flux $F^1_{i+1/2}$ and a first order robust numerical flux $F^L_{i+1/2}$:

$$F^*_{i+1/2} = (1 - \varphi^1_{i+1/2})F^L_{i+1/2} + \varphi^1_{i+1/2}F^1_{i+1/2}, \tag{18}$$

where $\varphi_{i+1/2}$ is a standard flux limiter function: Minmod, Superbee, Van Albada etc.

- Order $1 - 2$.
- Low computational cost.
- Diffusive near critical points.

The Adaptive Compact Approximation Taylor **ACAT** methods, introduced by Carrillo, Macca, CP, Russo, Zorío [2], are based on a combination of a robust first-order scheme and the Compact Approximate Taylor methods of order $2p$, $p = 1, 2, \ldots, P$ so that they are first-order accurate near discontinuities and have order $2p$ in smooth regions, where $(2p + 1)$ is the size of the biggest stencil in which data are smooth according to the smoothness indicators.

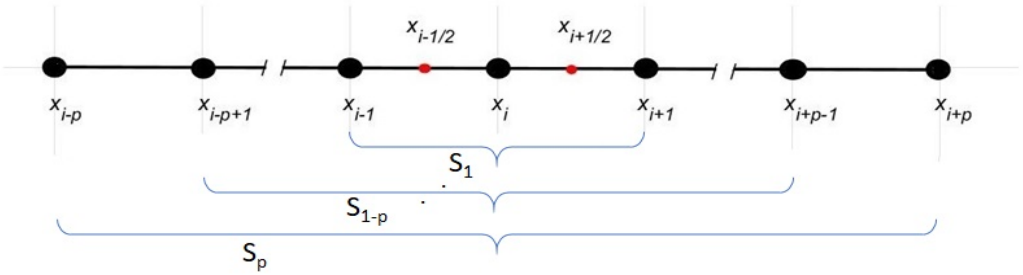

The strategy to be followed here consists on selecting automatically the stencil used to compute $F_{i+1/2}$ so that its length is maximal among those for which the solution is smooth.

More specifically, let us suppose that solutions $\{u_i^n\}$ at time t^n have been computed. The maximum length of the stencil to compute $F_{i+1/2}$ is set to, say, $2P$, where P is a natural number. Then, the candidates stencils to compute $F_{i+1/2}$ are

$$S_p^{i+1/2} = \{x_{i-p+1}, \ldots, x_{i+p}\}, \quad p = 1, \ldots, P.$$

In order to select the stencil, some smoothness indicators $\psi_{i+1/2}^p, \quad p = 1, \ldots, P$ are computed such that:

$$\psi_{i+1/2}^p \approx \begin{cases} 1 & \text{if } \{u_i^n\} \text{ is 'smooth' in } S_p^{i+1/2}, \\ 0 & \text{otherwise.} \end{cases} \tag{19}$$

Define now:

$$\mathcal{A} = \{p \in \{1, \ldots, P\} \; s.t. \; \psi_{i+1/2}^p \cong 1\}.$$

The idea would be then to define:

$$F_{i+1/2}^A = \begin{cases} F_{i+1/2}^{lo} & \text{if } \mathcal{A} = \emptyset; \\ F_{i+1/2}^{p_s} & \text{where } p_s = \max(\mathcal{A}) \text{ otherwise;} \end{cases}$$

where $F_{i+1/2}^{p_s}$ is the numerical flux of CAT2p_s and $F_{i+1/2}^{lo}$ is a robust first-order numerical flux.

Nevertheless, it is not possible to determine if the solution is smooth or not in the stencil $S_1^{i+1/2}$ where only two values u_i^n, u_{i+1}^n are available. Therefore, what will be done in practice is to define:

$$\mathcal{A} = \{p \in \{2, \ldots, P\} \; s.t. \; \psi_{i+1/2}^p \cong 1\}. \tag{20}$$

and then:

$$F_{i+1/2}^A = \begin{cases} F_{i+1/2}^* & \text{if } \mathcal{A} = \emptyset; \\ F_{i+1/2}^{p_s} & \text{where } p_s = \max(\mathcal{A}) \text{ otherwise;} \end{cases} \tag{21}$$

where $F_{i+1/2}^*$ is the numerical flux of the FL-CAT2

Given the nodal approximations f_i of a function f at the stencil S_p, $p \geq 2$, centered at $x_{i+1/2}$, first define the lateral weights:

$$I_{p,L} := \sum_{j=-p+1}^{-1} (f_{i+1+j} - f_{i+j})^2 + \varepsilon, \quad I_{p,R} := \sum_{j=1}^{p-1} (f_{i+1+j} - f_{i+j})^2 + \varepsilon, \tag{22}$$

where ε is a small quantity that is added to prevent the lateral weights to vanish when the function is constant. Next, compute:

$$I_p := \frac{I_{p,L} I_{p,R}}{I_{p,L} + I_{p,R}}. \tag{23}$$

Finally, define the smoothness indicator of the stencil of S_p by

$$\psi^p_{i+1/2} := \left(\frac{I_p}{I_p + \tau_p} \right), \tag{24}$$

where

$$\tau_p := \left(\Delta^{2p-1}_{i-p+1} f \right)^2. \tag{25}$$

Here, $\Delta^{2p-1}_{i-p+1} f$ represents the undivided difference of $\{f_{i-p+1}, \ldots, f_{i+p}\}$.

If data in the stencil S_p are smooth, then

$$I_{p,L} = O(\Delta x^2), \quad I_{p,R} = O(\Delta x^2), \quad \tau_p = O(\Delta x^{4p}).$$

Since

$$\frac{1}{I_p} = \frac{1}{I_{p,L}} + \frac{1}{I_{p,R}}$$

then $I_p = O(\Delta x^2)$ and thus

$$\psi^p_{i+1/2} = \frac{I_p}{I_p + \tau_p} = \frac{O(\Delta x^2)}{O(\Delta x^2) + O(\Delta x^{4p})}$$

is expected to be close to 1.

On the other hand, if there is an isolated discontinuity in the stencil (say, at the left) then

$$\tau_p = O(1)$$

and

$$I_{p,L} = O(1), \quad I_{p,R} = O(\Delta x^2).$$

Since

$$\frac{1}{I_p} = \frac{1}{I_{p,L}} + \frac{1}{I_{p,R}}$$

then $I_p = O(\Delta x^2)$ and thus

$$\psi^p_{i+1/2} = \frac{I_p}{I_p + \tau_p} = \frac{O(\Delta x^2)}{O(\Delta x^2) + O(1)} \approx 0$$

is expected to be close to 0.

A rigorous analysis has been performed. Special care has to be taken if there is a critical point in the stencil.

Let us consider

$$u_t + u_x = 0$$

with initial condition

$$u_0(x) = 0.5 \sin(\pi x),$$

periodic boundary conditions, $CFL = 0.9$, 160 point mesh, $x \in [0, 2]$.

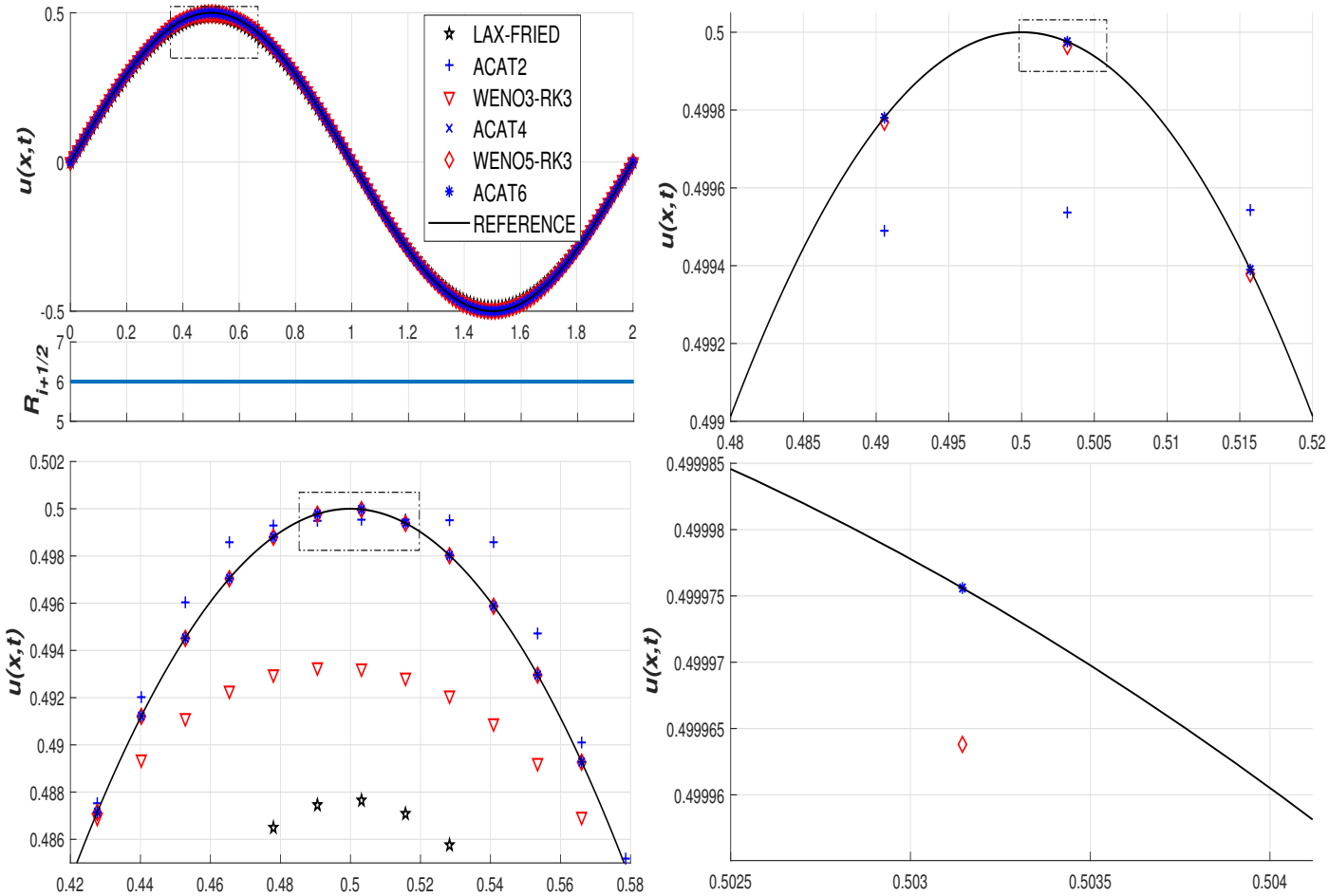

Numerical solution at $t = 4$: general view (*left-top*); local order of accuracy for ACAT6 (*sub-frame*); consecutive zooms close to the local maximum (*left-bottom*, *right-top* and *right-bottom*)

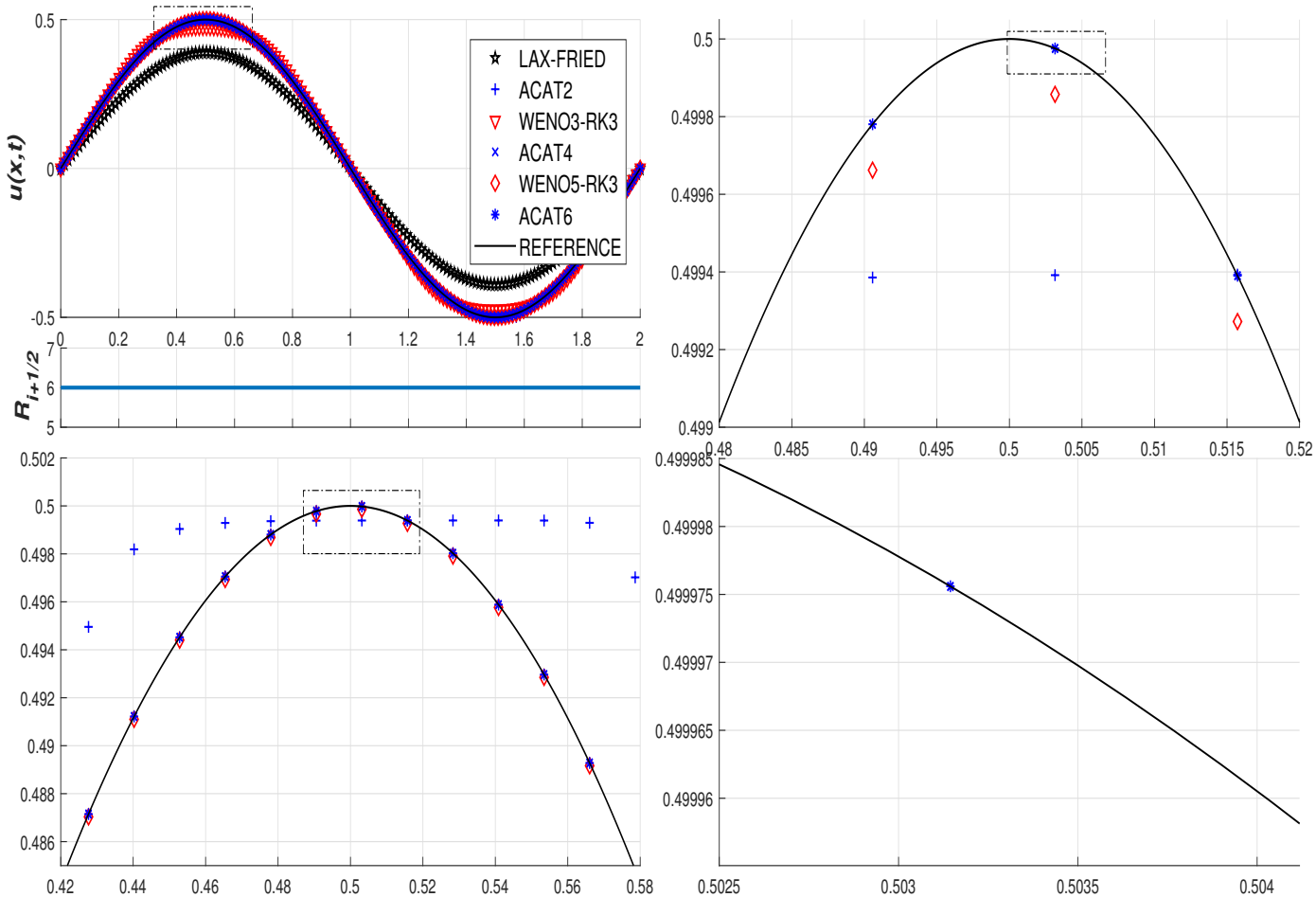

Numerical solution at $t = 40$: general view (*left-top*); local order of accuracy for ACAT6 (*sub-frame*); consecutive zooms close to the local maximum (*left-bottom*, *right-top* and *right-bottom*)

Let us consider

$$u_t + u_x = 0$$

with initial condition

$$u_0(x) = \begin{cases} 1 & \text{if } 1/2 \leq x \leq 1 \\ -1 & \text{if } 1 \leq x \leq 3/2 \\ 0 & \text{otherwise,} \end{cases}$$

periodic boundary conditions, $CFL = 0.9$, 160 point mesh, $x \in [0, 2]$.

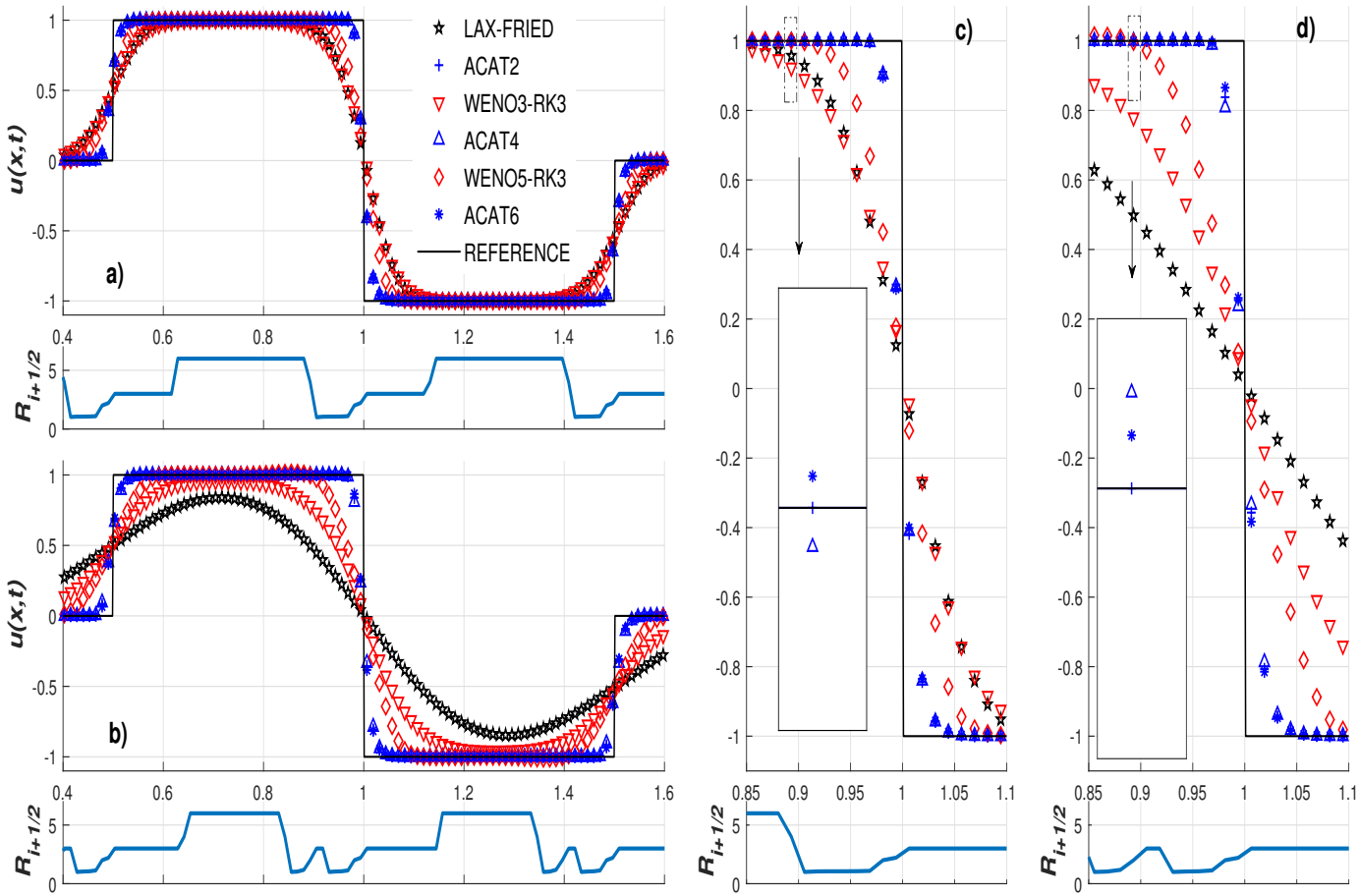

Numerical solutions at $t = 2$ (a) and $t = 20$ (b). Zoom of the numerical solutions at time $t = 2$ (c) and $t = 20$ (d). Sub-frames: local order of accuracy for ACAT6.

Let us consider

$$u_t + \left(\frac{u^2}{2}\right)_x = 0$$

with initial condition

$$u_0(x) = 0.5\sin(\pi x),$$

periodic boundary conditions, $CFL = 0.9$, 160 point mesh, $x \in [0, 2]$.

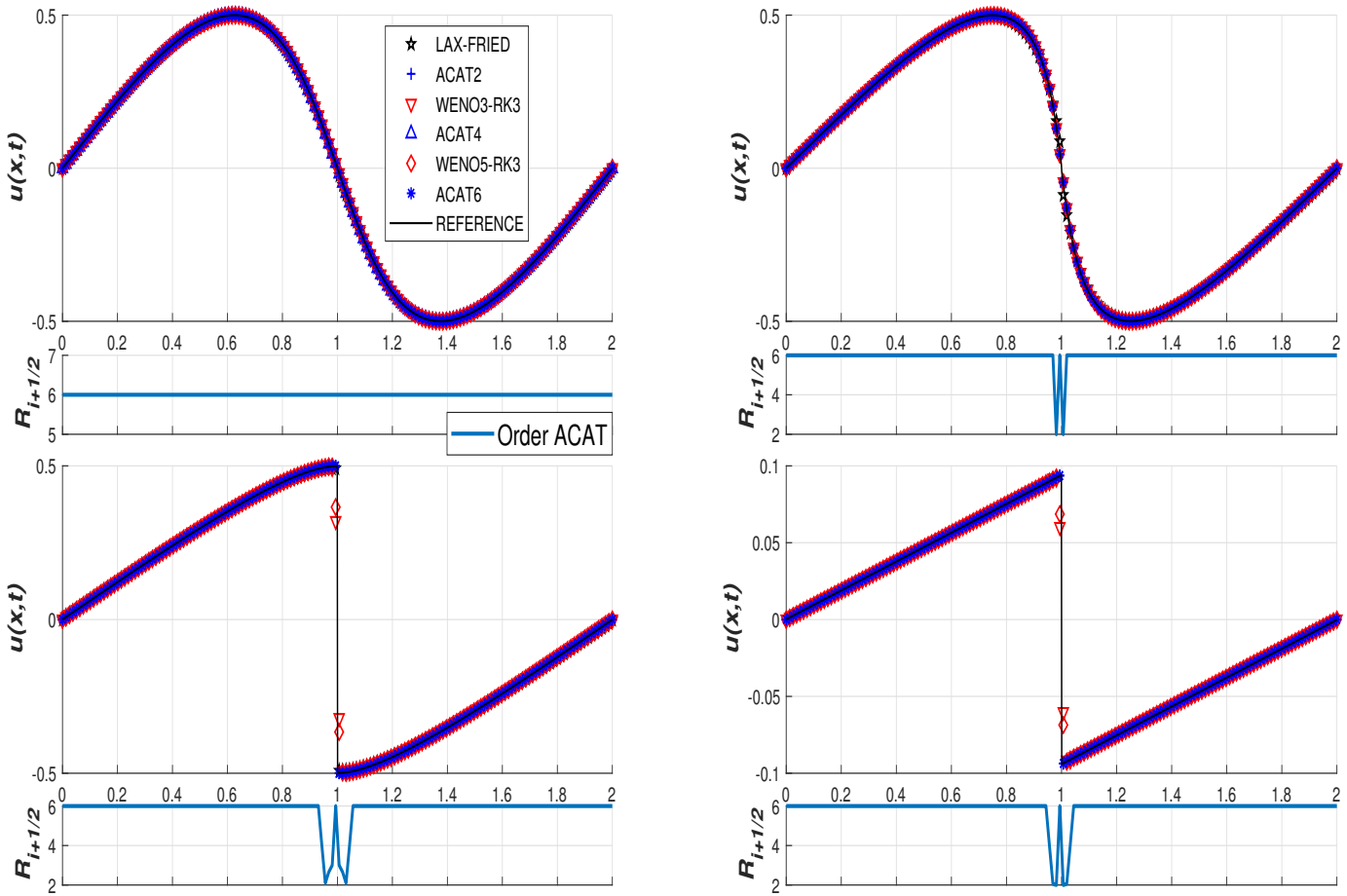

Numerical solutions obtained at times $t = 0.25$ (*left-top*), $t = 0.5$ (*right-top*), $t = 1$ (*left-bottom*), and $t = 10$ (*right-bottom*). Sub-frames: local order of accuracy for ACAT6.

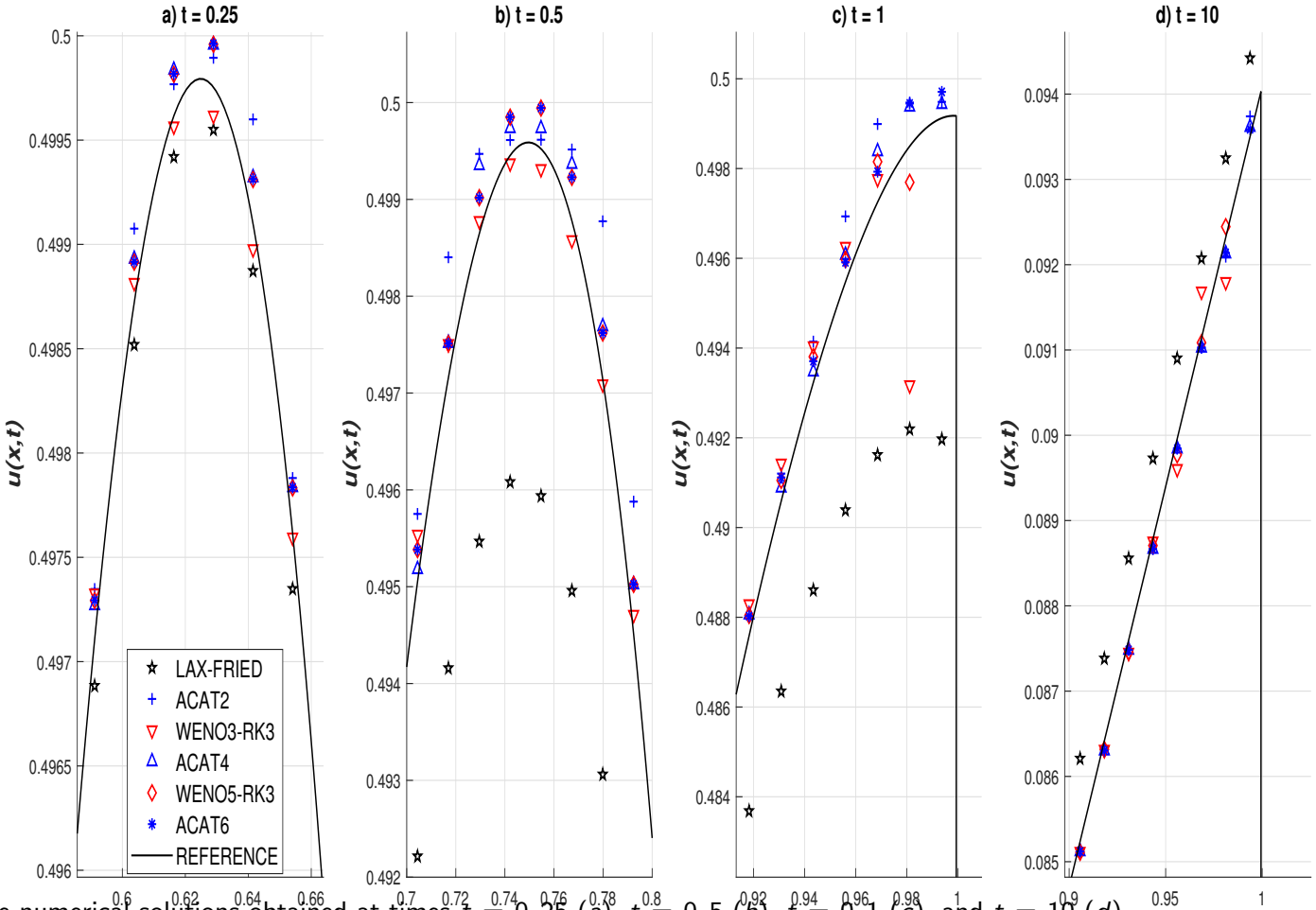

Zoom of the numerical solutions obtained at times $t = 0.25$ (a), $t = 0.5$ (b), $t = 0.1$ (c), and $t = 10$ (d).

We solve the $1d$ Euler equations for gas dynamics

$$\mathbf{u}_t + \mathbf{f}(\mathbf{u})_x = 0,$$

with

$$\mathbf{u} = \begin{pmatrix} \rho \\ \rho u \\ E \end{pmatrix}, \quad \mathbf{f}(\mathbf{u}) = \begin{pmatrix} \rho u \\ p + \rho u^2 \\ u(E+p) \end{pmatrix},$$

where ρ is the density, u the velocity, E the total energy per unit volume, and p the pressure. We assume an ideal gas with the equation of state,

$$p(\rho, e) = (\gamma - 1)\rho e,$$

being γ the ratio of specific heat capacities of the gas taken as 1.4 and e is the internal energy per unit mass given by:

$$E = \rho(e + 0.5u^2).$$

We solve the Sod problem using inflow-outflow boundary conditions, $CFL = 0.8$, 200 points mesh and $x \in [0, 1]$

$$(\rho, u, p) = \begin{cases} (1, 0, 1) & \text{if } x < 1/2, \\ (0.125, 0, 0.1) & \text{if } x > 1/2. \end{cases}$$

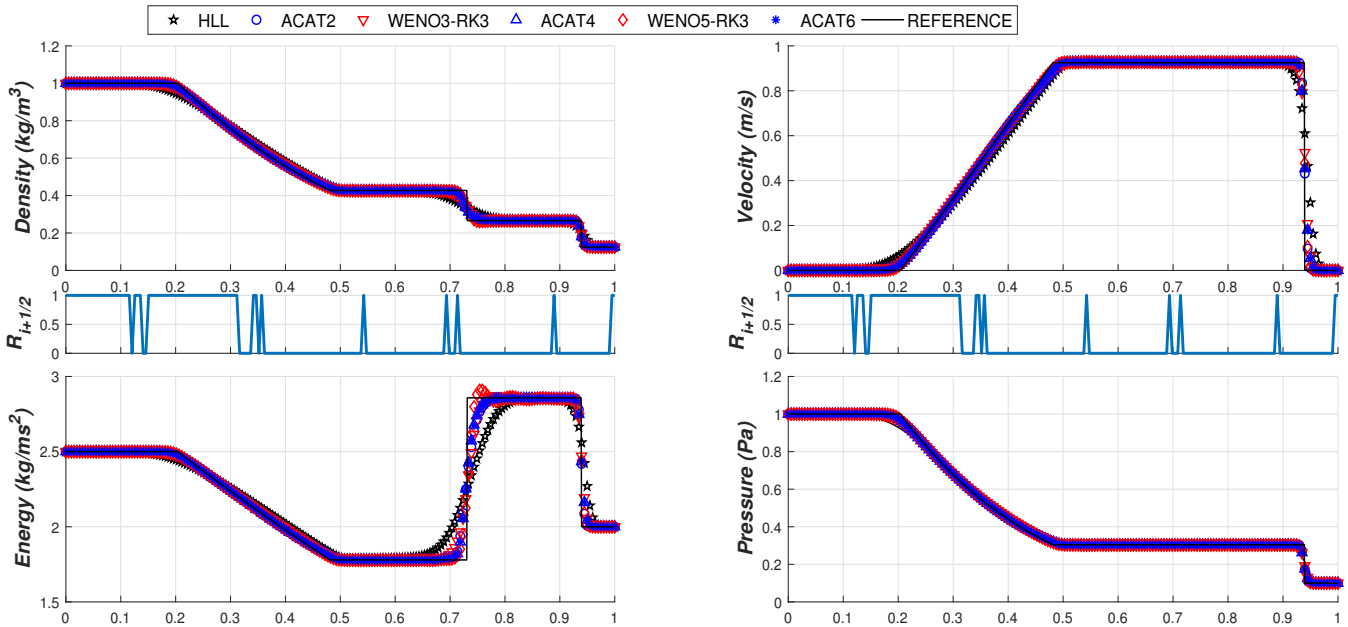

Zoom view, Density

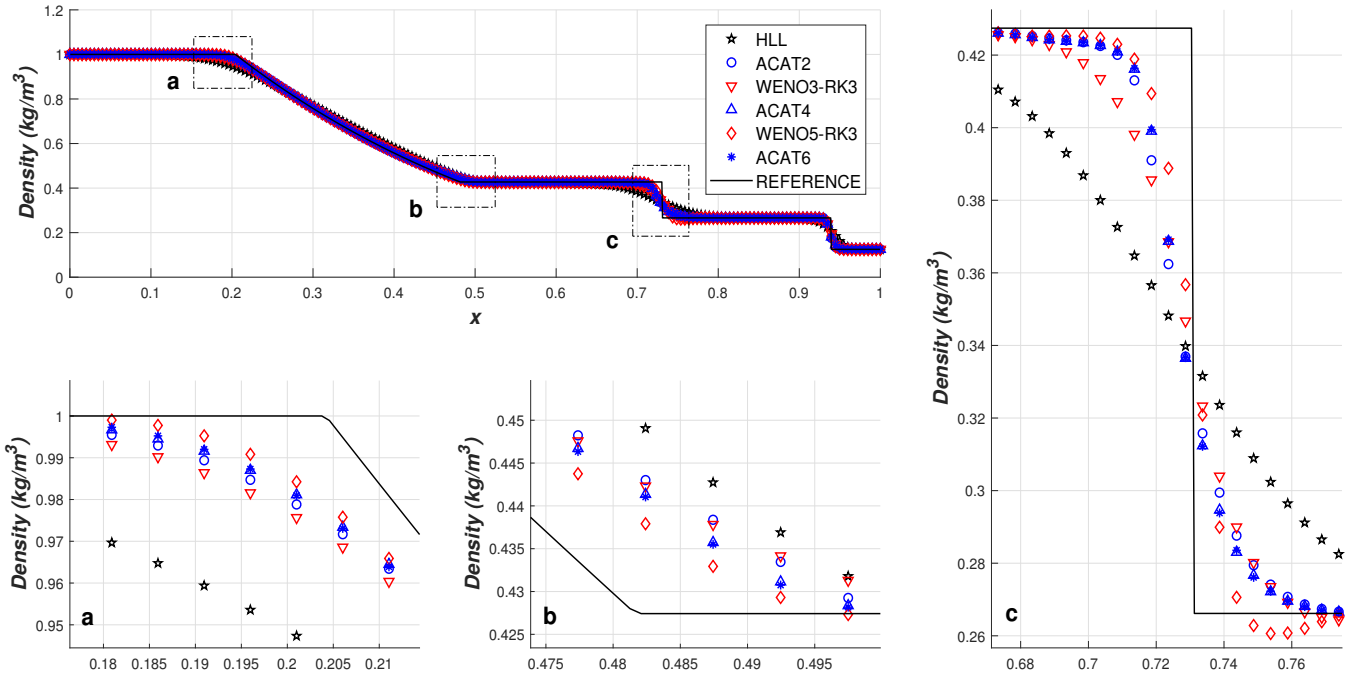

Zoom view, Energy

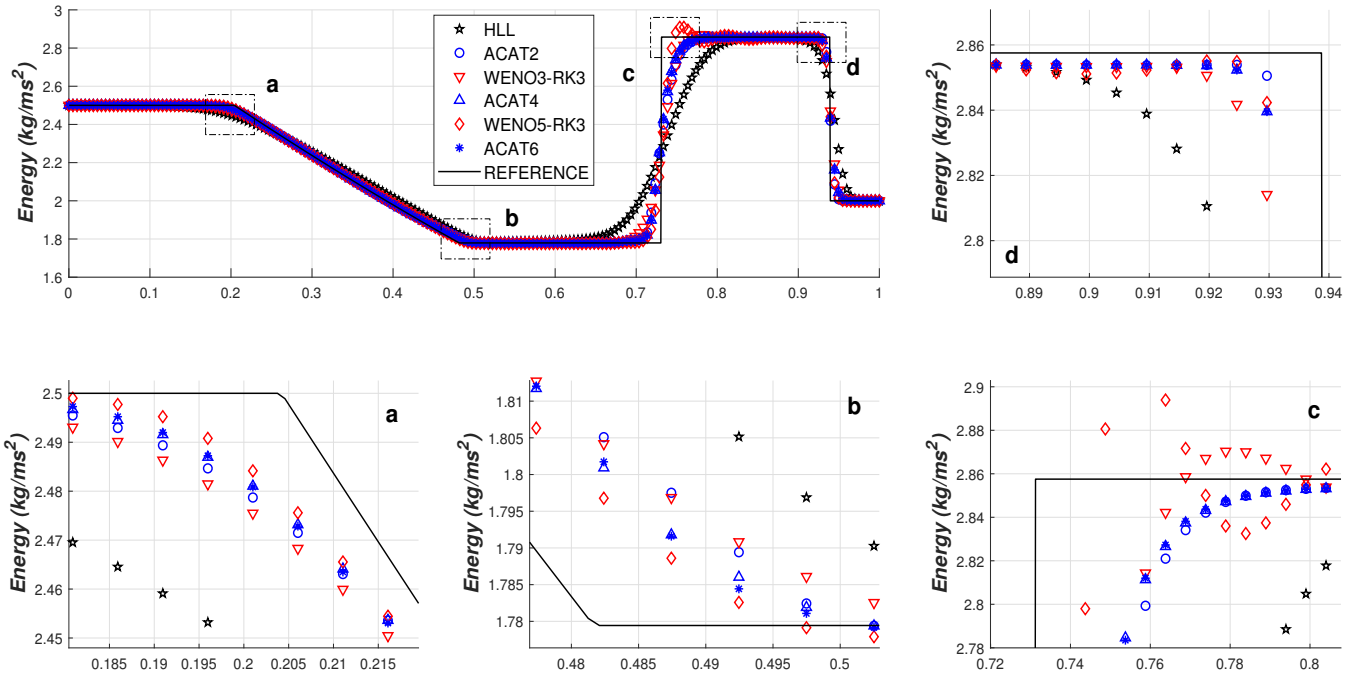

We consider now the two-dimensional Euler equations of gas dynamics:

$$\mathrm{w}_t + \mathrm{f}(\mathrm{w})_x + \mathrm{g}(\mathrm{w})_y = 0 \ , \tag{26}$$

where

$$\mathrm{w} = \begin{pmatrix} \rho \\ \rho u \\ \rho v \\ E \end{pmatrix}, \quad \mathrm{f}(\mathrm{w}) = \begin{pmatrix} \rho u \\ \rho u^2 + p \\ \rho uv \\ u(E+p) \end{pmatrix}, \quad \mathrm{g}(\mathrm{w}) = \begin{pmatrix} \rho v \\ \rho uv \\ \rho v^2 + p \\ v(E+p) \end{pmatrix}.$$

ρ is again the density; u, v are the components of the velocities in the x, y directions respectively; E, the total energy per unit volume; and p, the pressure. The equation of state

$$p(\rho, u, v, E) = (\gamma - 1)\left(E - \frac{\rho}{2}(u^2 + v^2)\right), \tag{27}$$

is assumed again where γ is the ratio of specific heat capacities of the gas.

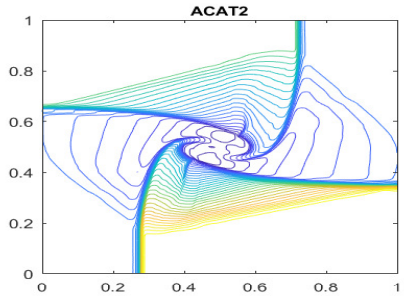
ACAT2

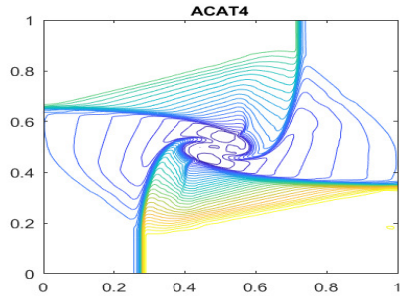
ACAT4

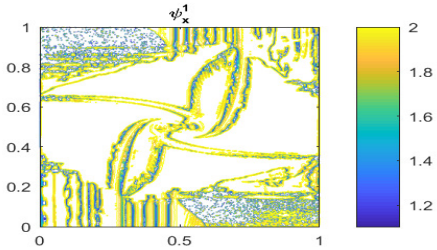
ψ_x^1

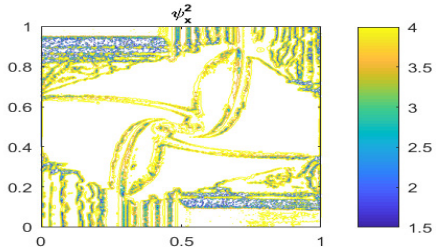
ψ_x^2

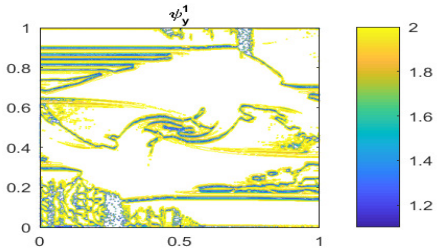
ψ_y^1

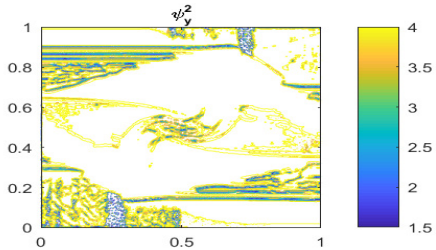
ψ_y^2

Comparison. Transport equation.

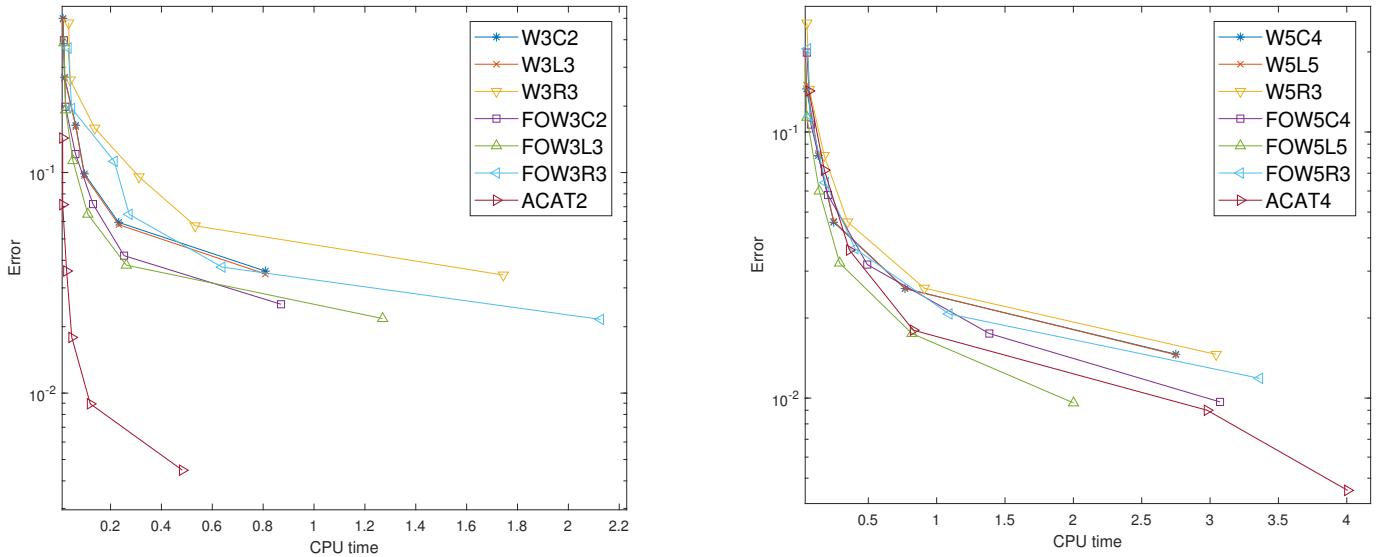

Linear transport equation: efficiency plot for WENO-CAT, WENO-LAT, WENO-RK, FOWENO-CAT, FOWENO-LAT, FOWENO-RK, and ACAT solutions at $t = 4$ and CFL$= 0.5$. Second and third-order methods (*left*). Fourth and fifth-order methods (*right*).

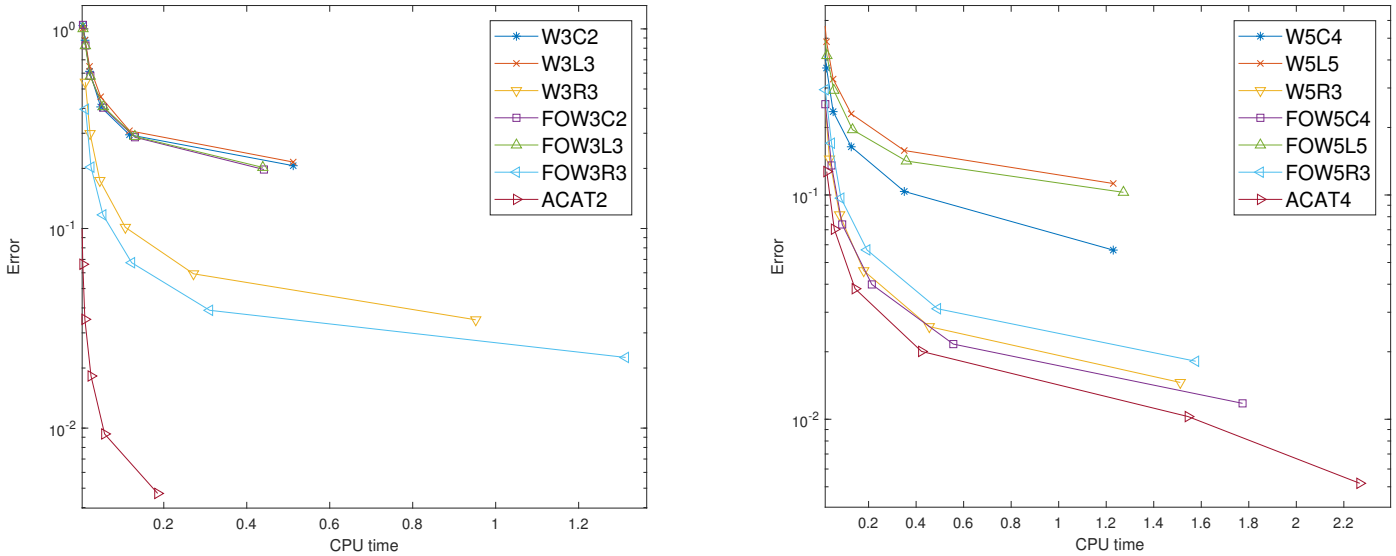

Linear transport equation: efficiency plot for WENO-CAT, WENO-LAT, WENO-RK, FOWENO-CAT, FOWENO-LAT, FOWENO-RK, and ACAT solutions at $t = 4$ and CFL$= 0.9$. Second or third-order methods (*left*). Fourth and fifth-order methods (*right*).

Some conclusions can be drawn:

- ACAT2 methods give the lowest errors for both CFL $= 0.5$ and 0.9, although it is only a second-order method.
- The error of all methods increase when CFL goes from 0.5 to 0.9, except for ACAT2 and ACAT4.
- For CFL $= 0.5$ ACAT2 is the most efficient method among those whose order of accuracy is 2 or 3. FOWENO5-LAT5 is the more efficient among those whose order is 3 or 5 followed by ACAT4.
- For CFL $= 0.9$ ACAT2 and ACAT4 are the most efficient methods.
- Efficient implementations of the methods in GPU architectures will be done to properly compare them.

Let us consider finally the 2D system of compressible Euler equations with a gravitational potential

$$\begin{cases} \rho_t + (\rho u)_x + (\rho v)_y = 0, \\ (\rho u)_t + (\rho u^2 + p)_x + (\rho uv)_y = -\rho H_x, \\ (\rho v)_t + (\rho uv)_x + (\rho v^2 + p)_y = -\rho H_y, \\ E_t + (u(E+p))_x + (v(E+p))_y = -\rho u H_x - \rho v H_y, \end{cases} \tag{28}$$

with equation of state

$$p = (\gamma - 1)\Big(E - \frac{1}{2}\rho(u^2 + v^2)\Big),$$

and

$$H(x,y) = \frac{1}{\sqrt{(x-\frac{1}{3})^2 + (y+\frac{1}{2})^2}}.$$

ACAT2, ACAT4 are applied to the problem as well as their well-balanced versions WBACAT2, WBACAT4 that exactly preserve the family of isothermal stationary solution is given by

$$\rho^*(\mathrm{x}) = C_1 e^{-H(\mathrm{x})} \geq 0; \quad p^*(\mathrm{x}) = C_1 e^{-H(\mathrm{x})} + C_2 \geq 0; \quad u^* = v^* = 0; \quad E^* = \frac{p^*}{\gamma - 1}. \tag{29}$$

The stationary solution of the family corresponding to $C_1 = 1$, $C_2 = 0$ is taken as initial condition. A (21×21)-point mesh and $CFL = 0.9$ are considered and the exact solution is imposed at all the sides through the ghost points.

Points	2D ACAT4				
	ρ	u	v	p	E
20	3.87E-5	3.09E-3	9.84E-4	1.38E-4	1.84E-4
40	9.74E-6	1.48E-3	4.48E-4	5.78E-5	4.68E-5
80	2.42E-6	7.23E-4	2.12E-4	2.65E-5	1.12E-5
160	6.07E-7	3.57E-4	1.03E-4	9.97E-6	2.95E-6

Table: Errors in L^1 norm for ACAT4 at time $t = 0.3$.

Points	2D WBACAT4				
	ρ	u	v	p	E
20	3.77E-17	2.05E-17	2.11E-17	5.16E-17	2.06E-16
40	3.59E-17	1.86E-17	2.02E-17	4.43E-17	1.77E-16
80	3.33E-17	1.81E-17	1.92E-17	4.04E-17	1.61E-16
160	3.23E-17	1.76E-17	1.85E-17	4.00E-17	1.60E-16

Table: Errors in L^1 norm for WBACAT4 at time $t = 0.3$.

The initial condition now represents a perturbation of the hydrostatic stationary considered in the previous test case:

$$\rho(x,0) = e^{-H(x)} + 0.04e^{-200(x-0.8)^2-200(y-0.7)^2}; \quad p(x,0) = e^{-H(x)}; \quad u(x,0) = v(x,0) = \tag{30}$$

The figure shows the differences between the numerical solutions provided by ACAT2, ACAT4, WBACAT2, WBACAT4 and a reference solution.

Extension to systems of balance laws: numerical examples

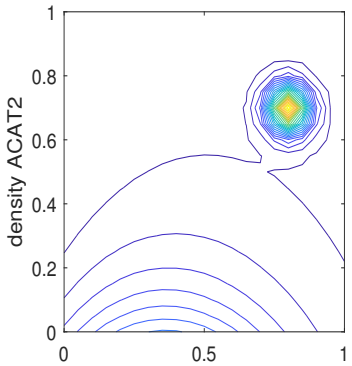

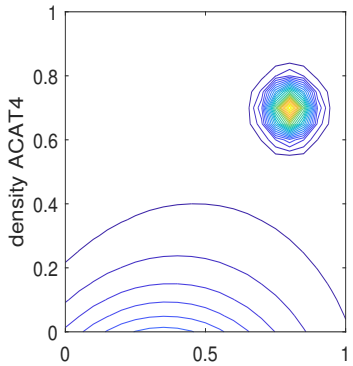

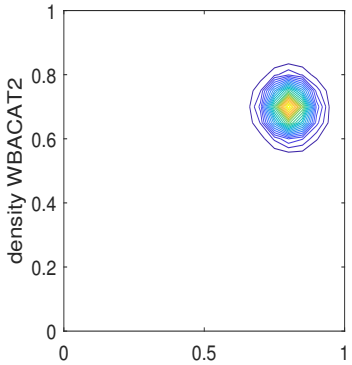

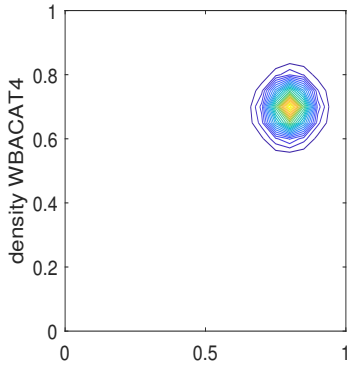

References

H. Carrillo and C. Parés.

Compact Approximate Taylor methods for systems of conservation laws.
Journal of Scientific Computing, 2019.

H. Carrillo, E. Macca, C. Parés, G. Russo, and D. Zorío.

An order-adaptive compact approximation Taylor method for systems of conservation laws.
arXiv:2007.01416, [math.NA] 2020.

H. Carrillo, C. Parés, and D. Zorío.

Lax Wendroff approximate Taylor methods with fast and optimized weighted essentially non-oscillatory reconstructions.
arXiv:2002.084261 [math.NA] 2020.

References

V.A. Titarev and E.F.Toro.

ADER: Arbitrarily high order Godunov approach.
Journal of Scientific Computing, 2002.

C. Enaux and M. Dumbser and E.F. Toro.

Finite volume schemes of very high order of accuracy for stiff hyperbolic balance laws.
Journal of Computational Physics, 227, 2008.

M. Dumbser and D. Balsara and E.F. Toro and C.D. Munz.

A unified framework for the construction of one-step finite-volume and discontinuous Galerkin schemes.
Journal of Computational Physics, 2008.

P. Lax and B. Wendroff.

Systems of conservation laws
Communications Pure and Applied Mathematics, vol 3. number 2, 1960.

J. Qiu and C.-W. Shu.

Finite difference WENO schemes with Lax-Wendroff-type time discretizations
SIAM Journal on Scientific Computing, 2003.

D. Zorío and A. Baeza and P. Mulet.

An approximate Lax–Wendroff-type procedure for high order accurate schemes for hyperbolic conservation laws.
Journal of Scientific Computing, 2017.

References

B. Fornberg.

Classroom note: calculation of weights in finte difference formulas.
SIAM Reviews, 1998.

Chi W. Shu.

Essentially Non-Oscillatory and Weighted Essentially Non–Oscillatory Schemes for Hyperbolic Conservation Laws.
Institute for Computer Applications in Science and Engineering (ICASE), 1997.

A. Baeza and R. Bürger and P. Mulet and D. Zorío

On the efficient computation of smoothness indicators for a class of WENO reconstructions,
Journal of Scientific Computing, 2019.

A. Baeza and R. Bürger and P. Mulet and D. Zorío.

WENO reconstructions of unconditionally optimal high order.
SIAM Journal on Numerical Analysis, 2019